Astron. & Astrophys. 40, 365—371 (1975)

# Scientific Instrumentation of the Radio-Astronomy-Explorer-2 Satellite

J. K. Alexander, M. L. Kaiser, J. C. Novaco, F. R. Grena and R. R. Weber
Laboratory for Extraterrestrial Physics, Goddard Space Flight Center

Received February 18, revised March 17, 1975

**Summary.** The RAE-2 spacecraft has been collecting radio astronomical measurements in the 25 kHz to 13 MHz frequency range from lunar orbit since June, 1973. This paper presents a summary of the technical aspects of the program and illustrates the performance of the experiments over the first 18 months of the flight. Among the unique features of the RAE-2 is the capability to observe repeated lunar occultations of strong radio sources at very low frequencies.

**Key words:** radio astronomy — space astronomy — instrumentation

## 1. Introduction

The Radio-Astronomy-Explorer-2 satellite was placed into lunar orbit on 15 June, 1973, to provide radio astronomical measurements of the planets, the Sun, and the Milky Way over the frequency range of 25 kHz to 13.1 MHz. In this paper, we discuss the characteristics of the RAE-2 instrumentation in order to provide the background of technical details necessary for a full understanding of the scientific results obtained with the satellite data. Since RAE-2 is in many ways practically identical to RAE-1, we will concentrate on those areas where the two spacecraft are significantly different and refer the reader to an earlier discussion of the RAE-1 spacecraft (Weber *et al.*, 1971) for further details and background on those items common to both satellites.

Among the major unexpected results from the four years of observations with the RAE-1 satellite (in Earth orbit) was the fact that radio emissions from the Earth—both natural and man-made—were very common and often very intense ($\geqq 40$ dB above the cosmic noise background) over the satellite experiment frequency range of 0.2 to 9.2 MHz. The second satellite in the RAE series was modified to be operated in lunar orbit where the terrestrial interference signals would be significantly weaker in general and completely eliminated during occultation periods. Some improvements were made to the scientific experiments to take advantage of the wider frequency range afforded by the low interplanetary plasma density, to provide for observations with higher time resolution than RAE-1, and to implement other changes based on experience with the performance of the RAE-1 instruments.

## 2. General Description

Like RAE-1, the RAE-2 antenna systems are comprised of a pair of long, travelling-wave *V*-antennas deployed from opposite sides of the spacecraft body to form an *X*-configuration and a 37-m dipole which is extended along the minor symmetry axis of the system as shown in Fig. 1. Gravity gradient forces stabilize the spacecraft so that the upper *V*-antenna is always pointed away

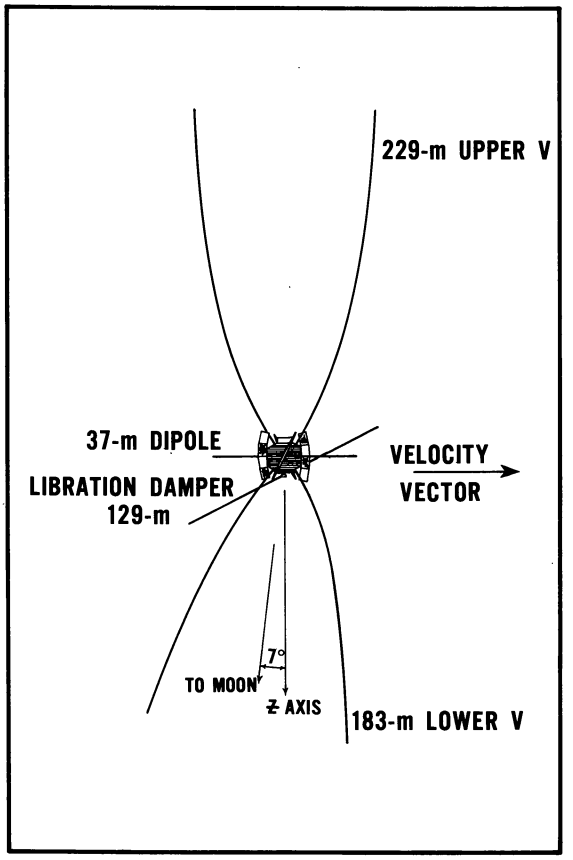


Fig. 1. Diagram of the RAE-2 boom configuration during the first sixteen months of operation. The lower *V*-antenna booms were extended to their full 229-m length in November, 1974

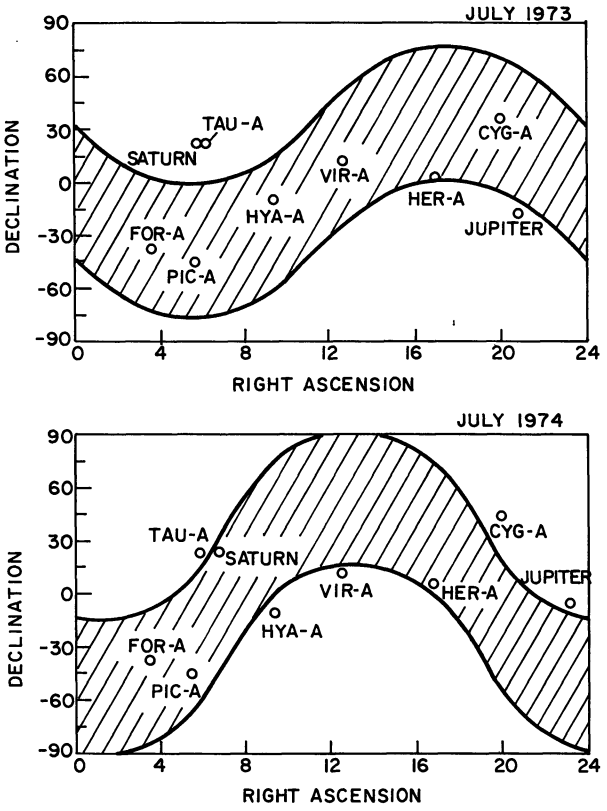


Fig. 2. Projection of the RAE-2 orbit in celestial coordinates showing that portion of the sky occulted by the Moon during the first year of the mission

from the Moon to scan the celestial sphere and the lower *V*-antenna is always directed downwards toward the Moon. A fourth boom system—a 129 m libration damper—is not utilized as an antenna but provides for damping of any spacecraft oscillations about the equilibrium position. The upper *V*-antenna is 229 m long and has an equivalent apex angle of 35°. Due to a mechanical flaw in one leg of the lower *V*-antenna which caused that leg to deploy nearly parallel to the local vertical, the lower *V*-antenna is asymmetrical in shape and was extended to a length of only 183 m during the first sixteen months of the flight before being deployed to 229 m in Nov. 1974. The asymmetry in the shape of the lower *V*-antenna results in a small angle between the spacecraft *z*-axis and the local vertical ($\sim 10°$) and a similar offset of the direction of maximum gain of the lower *V* (Sayre, 1975).

RAE-2 is in a circular orbit having an altitude of 1100 km, an inclination of 59° to the lunar equator, and a period of 222 m. Figure 2 shows two views of the celestial sphere as seen from the spacecraft in July of 1973 and 1974. The shaded areas are the regions occulted by the Moon during an orbit. Because of the upper-*V*/lower-*V* symmetry, the shaded areas also indicate the portion of the sky scanned with the upper-*V* during an orbit. These two views, separated by one year, illustrate how sky coverage is obtained through a combination of orbital scans and precession of the orbit plane at a rate of $-0.14°$/day relative to the lunar equator. During the first year of operation, this translated into precession of $-4.3$ h in right ascension and $+15°$ in declination. Occultations of Jupiter began occurring once each orbit on Aug. 13, 1973, and continued until June 19, 1974. Occultations of Saturn began Apr. 2, 1974. Earth occultations occur for about seven days out of every 14 days and last up to 48 m each orbit. During these periods, data are recorded on the spacecraft tape recorder for playback when the satellite is in view.

For the first three weeks of RAE-2 operation beginning on 20 June, 1973, only the short, 37-m dipole antenna was deployed. During this period, the satellite was operated in a spin-stabilized mode (at 4 rpm) with the spin axis located in the ecliptic plane and normal to the spacecraft-Sun line. Spin modulation effects observed on solar radio bursts during this phase of the mission provided the first information on the positions of low-frequency solar sources out of the ecliptic plane. Subsequently, the dipole booms were retracted, the spacecraft was reoriented, the long *V*-antennas and libration damper were extended, and the dipole was redeployed.

## 3. Antennas

The electrical properties of the travelling-wave *V*-antenna derived from theoretical studies, scale model measurements, and in-flight measurements in support of the RAE-1 mission are summarized by Weber *et al.* (1971) and by Alexander and Novaco (1974). The most detailed analytical studies of the radiation properties of the RAE-2 antennas have been performed by Sayre (1974), and a summary of the principal features of the calculated *V*-antenna radiation patterns over the RAE-2 frequency range is given in Table 1. The solid angle of the main lobe varies from the order of a steradian above a few MHz, to approximately a hemisphere near 1 MHz, to nearly isotropic at the lowest frequencies where the antenna is short compared with a wavelength. Scans of

Table 1. Summary of the radiation characteristics of the 229-m *V*-antenna

| Freq. | $\theta_E$ (FWHM) | $\theta_H$ (FWHM) | 1st Side lobe | Front: back |
|---|---|---|---|---|
| 9.18 MHz | 37° | 61° | − 2 dB | ~10 dB |
| 6.55 | 27 | 55 | − 4 | ~15 |
| 3.93 | 80 | 63 | − 5 | ~15 |
| 1.31 | 180 | 120 | −12 | ~15 |
| 0.87 | 220 | 160 | — | ~15 |

the Earth by the upper *V*-antenna at frequencies above the average nighttime ionospheric critical frequency generally confirm the theoretical estimates of the main beam size.

Theoretical analyses of the RAE-2 dipole antenna impedance (Sayre, 1974) show that the dipole radiation resistance is changed by interactions with the long *V*-antennas and libration damper boom. Corrections for this effect were applied to RAE-1 data by Weber (1972). Since the dipole was the first antenna extended on RAE-2, it has been possible to compare the changes in the dipole performance resulting from extension of the other booms by looking at apparent changes in the Galactic background radiation. When the long booms were extended, the dipole background levels increased at low frequencies and decreased at higher frequencies, confirming the predicted behavior.

## 4. Receivers

The receiving and calibration systems on RAE-2 are shown in the simplified block diagram in Fig. 3. The Ryle-Vonberg radiometers are essentially identical to those used on RAE-1 and normally make one frequency scan every 144 s. The burst receivers connected to each antenna are rapid sampling, total-power receivers which cover the 0.025 to 13.1 MHz range in 32 discrete steps. They have a bandwidth of 20 kHz and a post-detection time constant of 6 ms, and in the normal operating

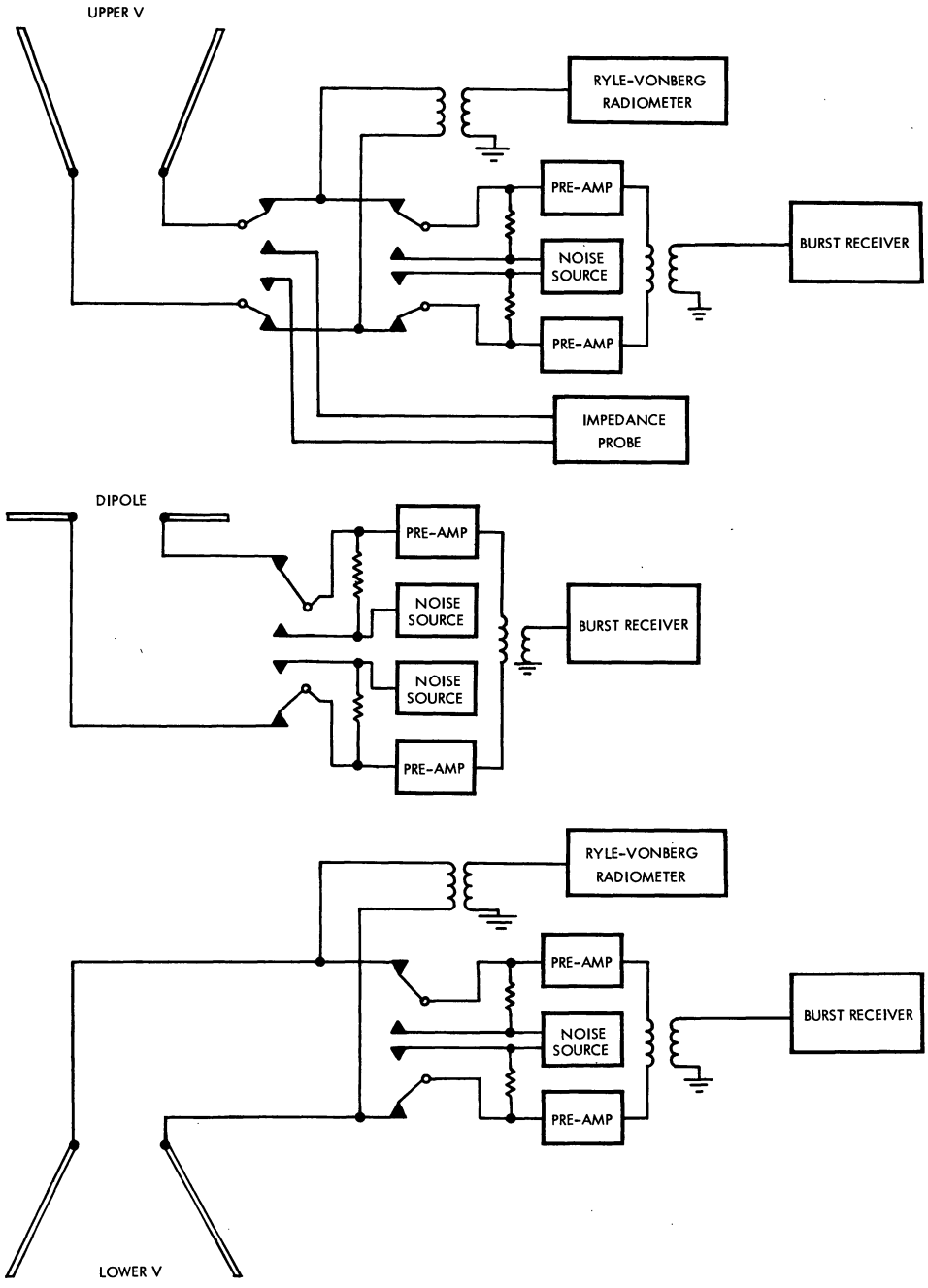


Fig. 3. Block diagram of the RAE-2 experiment instrumentation

mode, one frequency scan is made every 4 s on the dipole and every 8 s on the *V*-antennas. They are calibrated in flight once every 20 m by a noise source whose signal can be injected into the burst receiver preamps either in place of the antenna signal or in addition to the antenna signal through an isolation resistor. Each receiver has a total dynamic range of 60 dB which is divided into three 20-dB ranges for the Ryle-Vonberg radiometer and two 30-dB ranges for the burst receiver. Also every 20 m the upper *V*-antenna is connected to an impedance probe like that used on RAE-1. In-flight receiver performance has been very good to date. After correction for known temperature effects, the receiver data indicate that gain variations did not exceed $\sim 10\%$ during the first year of the flight.

## 5. Observations

The RAE-2 observations obtained from lunar orbit differ in character from the RAE-1 data in two important ways. At the lunar distance, RAE-2 is well separated from the emission regions of the Earth's magnetosphere and, thus, the Earth appears as an astronomical object in its own right. This can impose periodicities of 29.5 days (the lunar synodic month) and 24.8 h (the interval between consecutive sweeps of a given geographic position past the Moon) on the data at frequencies where the Earth is an active radio source. These striking noise enhancements are evident in Fig. 4 which displays the minimum antenna temperatures at selected frequencies recorded by the upper-*V* burst receiver during the last four months of 1973. Large increases in antenna temperature are seen at both high and low frequencies near each full Moon. Such enhancements were also observed by Grigoréva and Slysh (1970) with the Luna-11 and Luna-12 spacecraft. At 3.93 MHz, this is the time of maximum penetration of both man-made and thunder-storm radio noise (Herman and Stone, 1974) through the relatively transparent nighttime ionosphere. At the lower frequencies, radio emission caused by precipitating electrons in the auroral zones is at peak intensity at approximately 20–22 h geomagnetic local time on Earth (Gurnett, 1974). RAE-2 is essentially "above" this region just prior to full Moon. A similar, but much less intense type of auroral zone radio emission occurs near local noon or new Moon (Kaiser and Stone, 1975). The 24.8-h periodicity, most evident at 3.93 MHz, corresponds to passages of particular geographic coordinates past the sub-lunar point; whereas at the low frequencies, the auroral noise is related to the position of the geomagnetic pole as well as to local time.

Both the long-term stability of the receiving system and the available data coverage are also illustrated in Fig. 4. The slight change in level, particularly evident at 3.93 MHz in mid-November, results from the final *V*-antenna extension from 183 to 229 m.

The other, and perhaps more dramatic, difference between the RAE-2 and RAE-1 observations is the occurrence of lunar occultations of radio sources. As seen from the spacecraft, the Moon is a 76° diameter disk with a well defined edge. (The Earth as seen from RAE-1 had the same diameter but the "edges" of the Earth were not sharply defined or predictable because of gradients and inhomogeneities in the terrestrial ionosphere.) Source locations can be determined to a precision limited only by the uncertainty in calculation of the position of the lunar limb from ephemeris data. For worst case satellite ephemeris errors of $\pm 10$ s, the resultant position uncertainty is $\pm 15'$. Figure 2 shows the regions of the sky occulted at various times and the positions of some of the most intense discrete sources seen by ground-based radio telescopes. These sources will form a starting list of possible candidates for occultation events. However, the most impressive occultations are those of the Earth. The terrestrial noise sources referred to in Fig. 4 are seen on a much expanded time scale centered on an occultation of the visible Earth in Fig. 5. The top panel is a computer-generated dynamic spectral display of all 32 upper-*V* burst receiver channels with increasing intensity represented by increasing darkness. The auroral noise is the dark band running across the middle of the strip between 185 and 600 kHz. The lower panels show intensity-vs-time plots for several individual channels for the same period of time. The fact that the auroral noise does not disappear and reappear exactly coincident with the times of occultation of the visible Earth is evidence for the extended size of the source region. At the higher frequencies, however, the occultation of the thunderstorm and/or man-made noise occurs at the same time as the predicted geometrical occultation of the visible disk, confirming that this type of noise is generated at or near the Earth's surface.

The intense sporadic noise seen at the lowest few observing frequencies (below 100 kHz) in the dynamic spectrum is not diminished during Earth occultation, indicating a non-terrestrial origin. Grigoréva and Slysh (1970) observed diminutions of the high noise levels at 200 and 965 kHz when Luna-11 and Luna-12 were in lunar shadow, and they attributed this effect to shot noise generated by interaction of their 2.5-m antenna with the solar wind. Occasionally we also observe occultations of the very low frequency noise during solar eclipse; however we do not see any evidence for continuously enhanced noise levels above 100 kHz. This result is not incompatible with the findings from the Luna experiments since the much longer RAE-2 antennas are much less susceptible to shot noise effects (de Pazzis, 1969).

In addition to the Earth, occultations of the Sun (Fainberg, 1974) and Jupiter have been detected. The potential occultation candidates of Fig. 2 are much less intense radio sources and, thus, require rather sophisticated

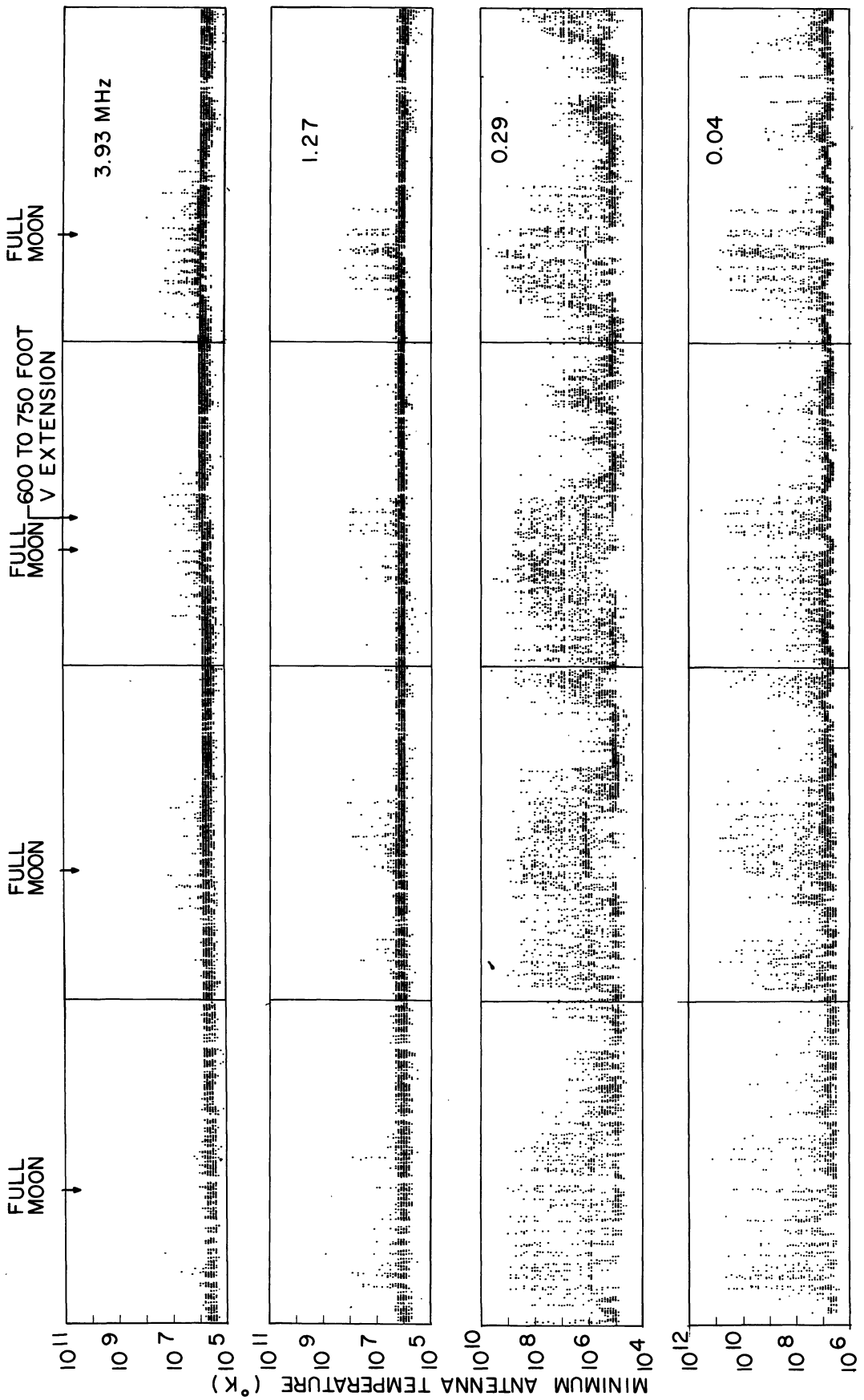


Fig. 4. Plot of the minimum signal level for each ten-minute interval observed at selected frequencies with the upper *V*-antenna during August through December, 1973

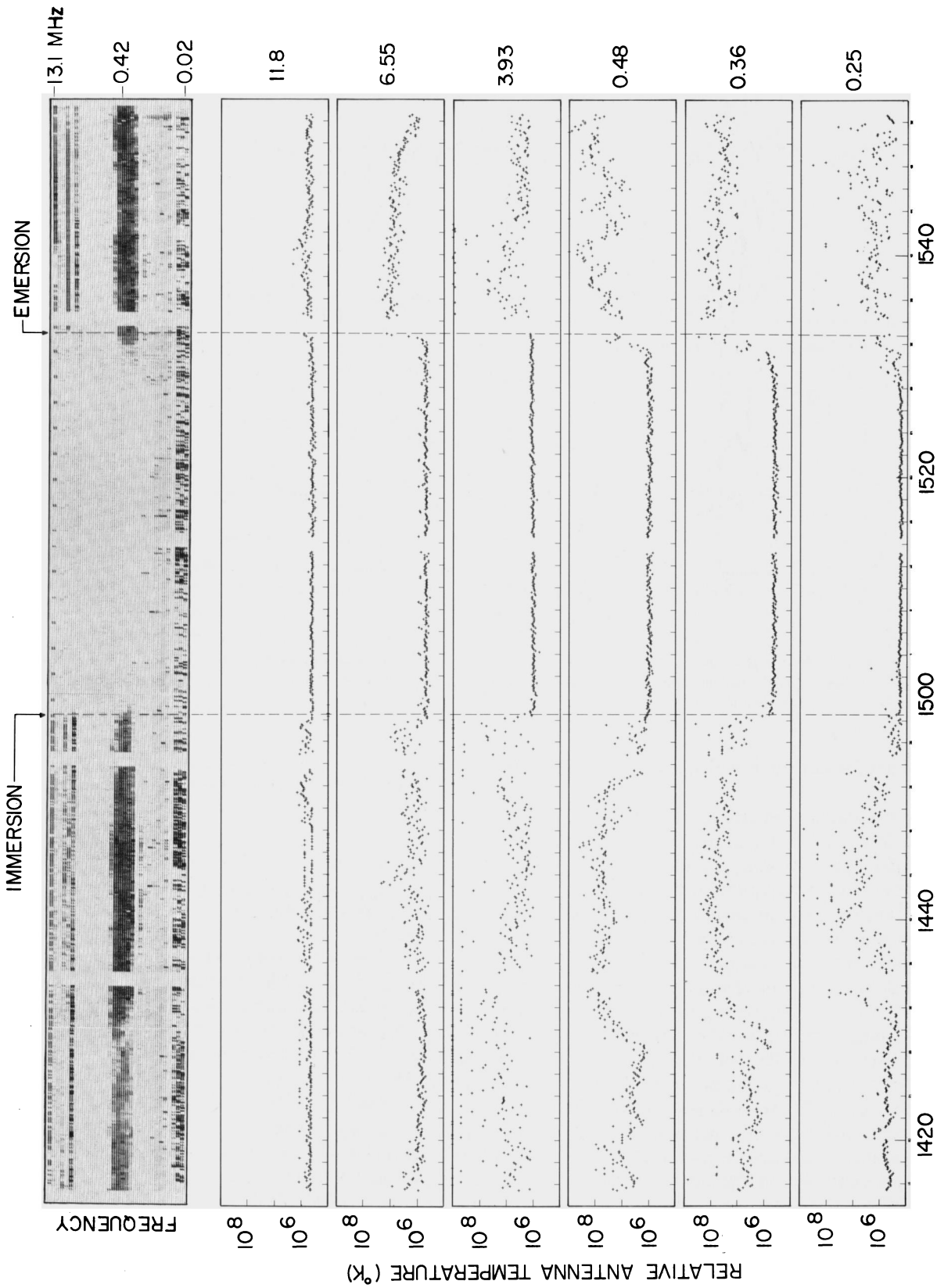


Fig. 5. Example of a lunar occultation of the Earth as observed with the upper-*V* burst receiver. The top frame is a computer-generated dynamic spectrum; the other plots display intensity vs. time variations at frequencies where terrestrial noise levels are often observed. The 80-s data gaps which occur every 20 m are at times when in-flight calibrations occur. The short noise pulses observed every 144 s at the highest frequencies during the occultation period are due to weak interference from the Ryle-Vonberg receiver local oscillator on occasions when both that receiver and the burst receiver are tuned to the same frequency

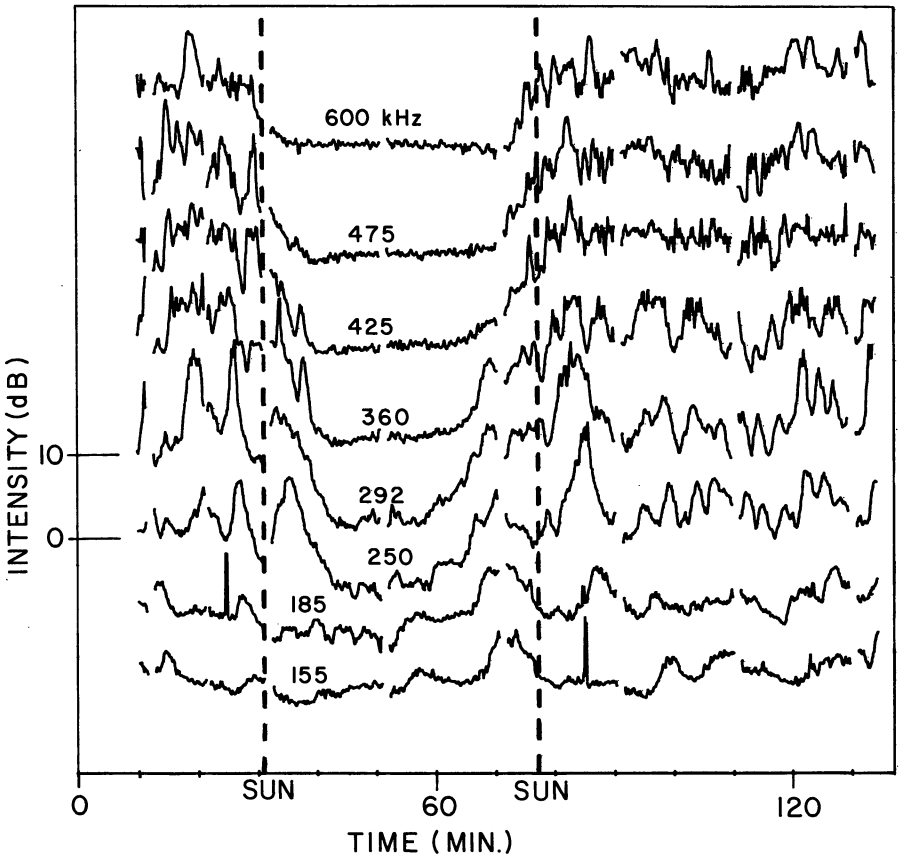


Fig. 6. Example of a lunar occultation of a solar storm (from Fainberg, 1974). The emission level scale derived from RAE-1 solar data (Fainberg and Stone, 1974) would predict that no clear occultation event should be observed below about 200 kHz since the apparent source size would exceed the size of the lunar disk as observed by RAE-2

averaging techniques for detection which are currently being developed.

Major observing programs with the RAE-2 are being conducted in the areas of Galactic astronomy, solar astronomy, and planetary astronomy. Observations of the Galactic background distribution with the 229-m upper *V*-antenna will supplement earlier RAE-1 measurements by providing wider frequency coverage ($\sim 1$ to 10 MHz) and new data at declinations above 60°. New information on the locations of solar radio sources between $< 10$ and 200 $R_\odot$ is becoming available from measurements of lunar occultations of solar bursts (Fig. 6). Enormous detail regarding the Earth as a low-frequency radio source is now available from the perspective of the lunar orbit. A comprehensive search for other radio sources including the planets, Galactic objects, and extragalactic sources is now under way, and with the optimism shared by all astronomers we can look for the greatest surprises to come from unpredicted results of that search.

*Acknowledgements.* A project as large and complex as RAE-2 depends on the efforts of many individuals for its success. We especially want to acknowledge the contributions of Project Manager J. T. Shea, Project Scientist R. G. Stone, our colleagues in the Radio Astronomy Branch who collaborated in all phases of the RAE-2 experiments and the talented engineers and technicians at Goddard who built the RAE-2 spacecraft and guided it into lunar orbit in good health.

## References

Alexander, J.K., Novaco, J.C. 1974, *Astron. J.* **79**, 777
Fainberg, J. 1974, Meeting of US National Committee of URSI, Boulder, Colorado
Fainberg, J., Stone, R.G. 1974, *Space Sci. Rev.* **16**, 145
Grigoréva, V.P., Slysh, V.I. 1970, *Kosmich. Issled.* **8**, 284
Gurnett, D.A. 1974, *J. Geophys. Res.* **79**, 4227
Herman, J.R., Stone, R.G. 1974, Meeting of US National Committee of URSI, Boulder, Colorado
Kaiser, M.L., Stone, R.G. 1975, Science (in press)
de Pazzis, O. 1969, *Radio Sci.* **4**, 91
Sayre, E.P. 1974, Meeting of US National Committee of URSI, Boulder, Colorado
Weber, R.R. 1972, *Astron. J.* **77**, 707
Weber, R.R., Alexander, J.K., Stone, R.G. 1971, *Radio Science* **6**, 1085

J. K. Alexander
M. L. Kaiser
J. C. Novaco
F. R. Grena
R. R. Weber
Code 693
Goddard Space Flight Center
Greenbelt, Md 20771, USA